Title Page

Simultaneous Assessment in vitro of Transporter and Metabolic Processes in Hepatic Drug Clearance: Use of a media loss approach

James Harrison, Tom De Bruyn, Adam S. Darwich, J. Brian Houston

Centre for Applied Pharmacokinetic Research, Division of Pharmacy and Optometry, School of Biology, Medicine and Health Sciences, University of Manchester, UK. (JH, TDB, ASD, JBH)

Department of Drug Metabolism and Pharmacokinetics, Genentech Inc, South San Francisco, CA, USA (TDB)

Running Title Page

Running Title: Media Loss Assay to Assess Metabolic and Transport Clearance

Corresponding Author:

J. Brian Houston

Centre for Applied Pharmacokinetic Research, Division of Pharmacy and Optometry, University of Manchester, M13 9PT, UK.

Telephone: +44 (0) 161-275-2358;

Fax: +44-161-275-8349).

E-mail address: brian.houston@manchester.ac.uk

Number of text pages: 21

Number of tables: 4

Number of figures: 6

Number of references: 28

Number of words in abstract: 250

Number of words in introduction: 614

Number of words in discussion: 1464

Non-standard Abbreviations (alphabetical order):

ABT (1-Aminobenzotriazole); CL_{active} (Active Uptake Clearance); CL_{int} (Intrinsic Clearance); $CL_{int,\ in\ vivo}$ (*In vivo* Intrinsic Clearance); $CL_{int,\ ML}$ (Media Loss Intrinsic Clearance); CL_{met} (Metabolic Intrinsic Clearance); $CL_{met,app}$ (Apparent Metabolic Intrinsic Clearance); CL_p (Plasma Clearance); $CL_{passive}$ (Passive Uptake Clearance); CL_{uptake} (Total Uptake Intrinsic Clearance); fu_b (Fraction of Unbound Drug in the Blood); fu_p (Fraction of Unbound Drug in the plasma); GMFE (Geometric Mean Fold

Error); Kp (Hepatocyte to Medium Partition Co-Efficient for Total Drug); Kp_u (Hepatocyte To Medium Partition Co-Efficient For Unbound Drug); Q_H (Hepatic Blood Flow); R_b (Blood to Plasma Ratio); Rfc (Rifamycin SV); RMSE (Root Mean Squared Error); V_{cell} (Volume of the Cell); $V_{cell,app}$ (Apparent Volume of the Cell); WME (Williams' Medium E).

Abstract

Hepatocyte drug depletion-time assays are well established for determination of metabolic clearance *in vitro*. The present study focuses on the refinement and evaluation of a “media loss” assay, an adaptation of the conventional depletion assay involving centrifugation of hepatocytes prior to sampling, allowing estimation of uptake in addition to metabolism. Using experimental procedures consistent with a high throughput, a selection of 12 compounds with a range of uptake and metabolism characteristics (atorvastatin, cerivastatin, clarithromycin, erythromycin, indinavir, pitavastatin, repaglinide, rosuvastatin, saquinavir and valsartan, with two control compounds - midazolam and tolbutamide) were investigated in the presence and absence of the cytochrome P450 inhibitor 1-aminobenzotriazole and organic anion transporter protein inhibitor rifamycin SV in rat hepatocytes. Data generated simultaneously for a given drug provided, through the use of a mechanistic cell model, clearance terms characterising metabolism, active and passive uptake, together with intracellular binding and partitioning parameters. Results were largely consistent with the particular drug characteristics, with active uptake, passive diffusion and metabolic clearances ranging between 0.4 – 777, 3 - 383 and 2 - 236 µL/min/mg protein, respectively. The same experiments provided total and unbound drug cellular partition coefficients ranging between 3.8 – 254 and 2.3 – 8.3, respectively and intracellular unbound fractions between 0.014 – 0.263. Following *in vitro* to *in vivo* extrapolation, the lowest prediction bias was noted using uptake clearance, compared to metabolic clearance or apparent clearance from the media loss assay alone. This approach allows rapid and comprehensive characterisation of hepatocyte drug disposition valuable for prediction of hepatic processes *in vivo*.

Introduction

An array of *in vitro* methodologies have been developed in order to measure permeability and metabolic properties of drugs and new chemical entities, however within the pharmaceutical industry there is more confidence in using the later than the former for predicting *in vivo* pharmacokinetics (Jones et al., 2015). Predicting *in vivo* hepatic clearance, due to metabolism alone, has matured over the last two decades (Houston, 1994, Wood et al., 2017) and is routinely applied. While the importance of transporters in controlling drug uptake and modulating metabolic enzyme interactions is widely appreciated (Chu et al., 2013, Giacomini et al., 2010, Shitara et al., 2006), standard *in vitro* and *in silico* approaches for assessment and extrapolation have yet to be broadly accepted (Zamek-Gliszczynski et al., 2013).

Uptake assays can be performed *in vitro* using multiple formats, however methods are typically labour intensive. The classic oil-spin approach uses hepatocytes in suspension, requiring incubations to be centrifuged through a layer of oil to allow the separation of cells and media (Miyauchi et al., 1993, Hallifax and Houston, 2006). Monolayer and sandwich cultured hepatocyte formats have also been developed which offer certain advantages, and can be used to generate similar estimates of uptake (De Bruyn et al., 2013, Menochet et al., 2012). However, these systems require hours/days of culture time before drug assays can commence. It is argued that during this delay transporter expression at the membrane declines, which may lead to under prediction of clearance (Jigorel et al., 2005). The decline in P450 activity with time is also well documented (Griffin and Houston, 2005, Paine, 1990), and must be another consideration for these formats. The “media loss” assay was developed (Soars et al., 2007) to provide a more rapid experimental option for determining drug uptake, and

retains many similarities to metabolic stability assays (subsequently referred to as the "conventional" assay). The course of drug depletion is monitored over time and from the simultaneous use of the media loss (involving the centrifugation of cells prior to sampling) and the conventional assay (involving direct sampling from the cell suspension) estimation of uptake and metabolism is achieved, making it possible to determine the likely rate-determining step in the hepatic clearance of the drug in question (Jigorel and Houston, 2012, Soars et al., 2007).

The primary restriction to the widespread use of uptake assays remains their labour intensive nature. The aim of this study, therefore, was to increase the throughput of the media loss assay, allowing the use of inhibitors of both uptake transporters and metabolic enzymes. Subsequently, a simple mechanistic model is used to determine several key pharmacokinetic parameters and to scale the *in vitro* parameters to determine the utility of this method for predicting *in vivo* hepatic clearance. Literature data for drug uptake data and metabolism rates in rat hepatocytes were used to identify a group of potential drugs for study. Figure 1 summarises the parameters reflecting active transport importance (assessed relative to passive transport with the parameter Kp_u) and metabolic clearance (CL_{met}) for 17 drugs. Ten compounds were selected for investigation which covers a range of properties: atorvastatin, cerivastatin, clarithromycin, erythromycin, indinavir, pitavastatin, repaglinide, rosuvastatin, saquinavir and valsartan. An additional two drugs selected for study (midazolam and tolbutamide) intended to act as control compounds. For these two drugs the role of hepatic transporters is minimal and hence Kp_u close to unity (Brown et al., 2007, Nicholls and Houston, 1996). Their differing rates of metabolism (tolbutamide being low clearance and midazolam high clearance) provide useful checks for the temporal

changes for both assay formats. The inhibitors selected for study were 1-aminobenzotriazole (ABT) for P450 (Mugford et al., 1992) and rifamycin-SV (Rfc) for Oatp1, Oatp2 and Ntcp (Fattinger et al., 2000).

Materials and Methods

Chemicals. Atorvastatin, indinavir, pitavastatin calcium, rosuvastatin and valsartan were purchased from Sequoia Research Products (Pangbourne, UK). Saquinavir and midazolam were purchased from Roche Products Ltd (Welwyn Garden City, UK). ABT, Rfc, clarithromycin, erythromycin, tolbutamide, and Bradford reagent were purchased from Sigma-Aldrich (Dorset, UK). Cerivastatin and repaglinide were purchased from Carbosynth Limited (Berkshire, UK). Phenol Red Free Williams' Media E (WME) was purchased from Lonza Ltd (Basel, Switzerland). All other reagents were obtained from Life Technologies (Paisley, UK).

Animal Source, Housing, and Diet. Male Sprague-Dawley rats (240–260g) were obtained from the Biological Sciences Unit, Medical School, University of Manchester (Manchester, UK). They were housed in groups of two in opaque boxes on a bed of sawdust in rooms maintained at a temperature of 20 ± 3°C, with a relative humidity of 40 to 70% and a 12-hour light/dark cycle. Animals were allowed free access to Chow Rat Mouse diet and fresh drinking water. All animal protocols were approved by the University of Manchester review committee.

Hepatocyte Isolation and Preparation. Rat hepatocytes were isolated from the livers of male Sprague-Dawley rats weighing between 250 – 300g (Charles River, Margate, Kent, UK). Rats were sacrificed using CO_2 overdose followed by cervical dislocation. Hepatocytes were prepared using an adaptation of the two-step collagenase perfusion method, as described previously (Berry and Friend, 1969). After isolation, hepatocytes were suspended in WME, as supplied by Lonza Ltd with no protein present, at pH 7.4. Cell count and viability were determined using the trypan blue exclusion method. Only

preparations exceeding 85% viability were used. Cells were diluted to a density of 2 x 10^6 cells/mL in WME before being split into aliquots. Inhibitors were added to the appropriate cell aliquots to give final concentrations of 1 mM ABT and 100 μM Rfc.

Conventional Depletion Assay. Cell suspensions (125 μL) were transferred to a 96-well plate and pre-incubated for 10 minutes in a Heidolph Inkubator 1000 (Heidolph, Schwabach, Germany) at 37°C and 900 rpm. Experiments were performed in duplicate and the maximum organic solvent concentration in the incubation was 0.11% (v/v). To initiate the reaction, 125 μL of drug solution (2 μM) in WME was added to the cell suspension. The final incubation, therefore, had a cell density of 1 x 10^6 cells/mL and a nominal drug concentration of 1 μM. At 9 specified time points, 75 μL aliquots were quenched in methanol containing relevant internal standard. Samples were stored at -20°C until analysis by liquid chromatography in tandem with mass spectrometry (LC-MS/MS). Cell suspensions were frozen overnight to lyse cells, and a Bradford protein assay (Biorad, Hemel Hempstead, UK) was performed to determine protein concentrations in each well.

Media Loss Assay. The media loss assay, described previously (Soars et al., 2007, Jigorel and Houston, 2012), was performed simultaneously with the conventional depletion assay. Methodology remained identical in both depletion assays, except for the addition of a centrifugation step immediately prior to sampling of the media. Adaptations were made to the protocols outlined by Jigorel and Houston (2012) and Soars et al. (2007) to allow the assay to be performed in 96-well plates. Hepatocyte density and volume, drug volume and shaking speed remained identical to that described by Jigorel and Houston (2012), while sampling volume was modified to 75

µL in order to maintain a sample to methanol ratio of 1:3, as described by Soars et al. (2007). Due to the limitations of the plate centrifuge and to minimise the delay from the desired time point to sample quenching, while maintaining sufficient separation of cells from the media, other differences in both protocols included the centrifugation speed (3000g) and time (15s), performed using an Eppendorf Centrifuge 5804 (Stevenage, UK).

LC-MS/MS Analysis. A Waters 2795 with a Micromass Quattro Ultima or Quattro Micro triple quadruple mass spectrometer (Waters, Milford, MA) was used for LC-MS/MS analysis. Analytes were centrifuged for 10 min at 2500 rpm and a 10 µL aliquot of the supernatant was analysed by LC-MS/MS. Four mobile phases (A, B, C and D) were used, the composition of each was as follows: A) 90% water; 10% methanol; 0.05% formic acid, B) 90% methanol; 10% water; 0.05% formic acid, C) 90% water; 10% methanol; 10 mM ammonium acetate, D) 90% methanol; 10% water, 10 mM ammonium acetate. A Luna C18 column (3 µm, 50 mm x 4.6 mm) or Luna Phenyl Hexyl column (5µm, 550 x 4.6 mm) was used for chromatographic separation of the analytes (Phenomenex, Torrance, CA), with the flow rate set at 1 mL/min split to 0.25 mL/min before entering the mass spectrometer.

Data Analysis and Modelling. Data were fitted to a monophasic or biphasic exponential decay model, described in Equation 1 and Equation 2,

$$C(t) = C_0 \cdot e^{-k \cdot t} \qquad \textbf{Equation 1}$$

where C_0 is the initial media substrate concentration and k is the elimination rate constant,

$$C(t) = A \cdot e^{-k_1 \cdot t} + B \cdot e^{-k_2 \cdot t}$$ **Equation 2**

where A and B represent the back-extrapolated drug concentration in the media in the first and second phase, respectively, and k_1 and k_2 are the elimination rate constants in the first and second phase, respectively. Following this, intrinsic clearance (CL_{int}) was calculated using Equation 3 and Equation 4 for monophasic and biphasic fits, respectively.

$$CL_{int} = \frac{V \cdot k}{P}$$ **Equation 3**

$$CL_{int} = \left(\frac{C_0 \cdot V}{\left(\frac{A}{k_1} + \frac{B}{k_2} \right)} \right) \Big/ P$$ **Equation 4**

Where V is the incubation volume and P is the amount of protein (mg) in each incubation. A single factor ANOVA and a post hoc Scheffe's test were used to determine if CL_{int} values were significantly different between conditions.

Figure 2 summarizes the experimental and data analysis methods used for data generated in the two assays. Panel A provides a schematic of the experimental steps taken and Panel B illustates the two-compartment mechanistic model used to describe drug uptake (active and passive), metabolism and distribution.

The latter was adapted from Jigorel and Houston (2012), implemented in Matlab R2014a (The MathWorks, Inc., Natick, MA) and produced estimates for the clearance

of active uptake (CL_{active}), bidirectional passive diffusion ($CL_{passive}$) and metabolism (CL_{met}; see Figure 2A and B). The mechanistic model was found to be most successful when using a step-wise approach and was not applied for drugs showing monophasic depletion under all conditions (midazolam and tolbutamide). In these cases active and passive uptake clearances in the media loss assay were practically unidentifiable.

The conventional assay was first modelled to obtain a measure of CL_{met}, as well as to obtain interaction terms for each inhibitor condition acting on CL_{met} (Int_{ABT}, Int_{Rfc} and Int_{ABTRfc}) described in Equation 5,

$$CL_{met,app} = CL_{met} \cdot Int_{ABT}^{ABT=0,1} \cdot Int_{Rfc}^{Rfc=0,1} \cdot Int_{ABTRfc}^{ABTRfc=0,1} \quad \textbf{Equation 5}$$

Where $CL_{met,app}$ is the apparent metabolic clearance, and ABT, Rfc and ABTRfc are power constants of 0 (in the absence of inhibitor) or 1 (in the presence of inhibitor). The default approach was to assume an additive effect of ABT and Rfc in the media loss assay, however in cases where the fitting was poor the combined ABTRfc term was implemented. CL_{met} is the non-saturable metabolic clearance term, with interaction terms acting as proportionality scalars to determine the overall effect in Equation 6. For the purpose of parameter identifiability, it was assumed that active transport was completely inhibited by Rfc at the concentrations used in this study (Fattinger et al., 2000). Parameters estimated based on the conventional assay were then fixed in the second step, where the media loss concentration-time profiles were modelled to estimate rates of CL_{active} and $CL_{passive}$ transport and the theoretical cell volume ($V_{cell, app}$). Total uptake clearance (CL_{uptake}) was calculated from the summation

of both CL_{active} and $CL_{passive}$. All results were normalised to the amount of protein within each well.

Differential equations Equation 6 (conventional assay), Equation 7 and Equation 8 (media loss assay) were used to describe the concentrations in both the cell and media over time.

$$\frac{dS_{med}}{dt} = \frac{-CL_{met} \cdot S_{med}}{V_{med}} \quad \textbf{Equation 6}$$

$$\frac{dS_{med}}{dt} = \frac{-(CL_{active} + CL_{passive} \cdot S_{med}) + (CL_{passive} \cdot S_{cell})}{V_{med}} \quad \textbf{Equation 7}$$

$$\frac{dS_{cell}}{dt} = \frac{(CL_{active} + CL_{passive} \cdot S_{med}) - (CL_{passive} + CL_{met} \cdot S_{cell})}{V_{app,cell}} \quad \textbf{Equation 8}$$

Where S_{med} is the concentration in the media, V_{med} is the experimental volume of the media (set at 250 µL) and S_{cell} is the concentration in the cell.

Other parameters were calculated as follows. Kp is the ratio of intracellular to media concentrations, and reflects the total drug within the cell, determined by passive permeation, active uptake and intracellular binding (Equation 9).

$$Kp = \frac{V_{app,cell}}{V_{cell}} \quad \textbf{Equation 9}$$

Where $V_{app,cell}$ is the apparent cellular volume of distribution, estimated using the mechanistic model, and V_{cell} is the intracellular volume, calculated assuming 3.9 µL/10^6 cells (Menochet et al., 2012) and a protein conversion of 1x10^6 cells/mg protein (determined in-house), multiplied by the amount of protein measured in each assay.

The ratio of unbound cytosolic drug concentrations, relative to the external medium, is described by the hepatocyte to medium partition co-efficient for unbound drug (Kp_u), and reflects the degree of active uptake (Equation 10).

$$Kp_u = \frac{CL_{active} + CL_{passive}}{CL_{passive}} \qquad \textbf{Equation 10}$$

where CL_{active} and $CL_{passive}$ are estimated by the mechanistic model. Due to evidence of internalisation of efflux transporters following hepatocyte isolation (Bow et al., 2008), efflux was assumed to be negligible. Finally, fu_{cell} was estimated using Equation 11.

$$fu_{cell} = \frac{Kp_u}{Kp} \qquad \textbf{Equation 11}$$

Prediction of *in vivo* clearance. For prediction of *in vivo* clearance, *in vitro* clearance parameters were scaled to whole body values of the rat using physiological scaling factors of 200 mg protein/g liver (Seglen, 1976) and 40 g liver/kg bodyweight (Davies and Morris, 1993). Data were scaled using protein content rather than cell number as this could be measured experimentally more accurately. For *in vivo* data, all blood clearance (CL_b) data were initially corrected for renal clearance. *In vivo* CL_{int} ($CL_{int,\ in\ vivo}$) was then calculated from *in vivo* CL_b, fraction of drug unbound in the blood (fu_b) and hepatic blood flow (Q_H, set at 100 mL/min/kg (Ito and Houston, 2004)) using the well-stirred model (Equation 12). Blood to plasma ratio (R_b) was used where necessary to calculate CL_b and fu_b from plasma clearance (CL_p) or fraction of drug unbound in the plasma (fu_p) using CL_p/R_b or fu_p/R_b, respectively. Mean values were

used when multiple sources were available. See Supplemental Table 2 for full list of values and references.

$$CL_{int,in\ vivo} = \frac{CL_b}{fu_b \cdot \left(1 - \frac{CL_b}{Q_H}\right)} \qquad \textbf{Equation 12}$$

Bias and precision of *in vitro* values were assessed using the absolute geometric mean fold error (GMFE, Equation 13) and the root mean squared error (RMSE, Equation 14), respectively (Hallifax et al., 2010). Qualitative assessment of predictions were judged as being well predicted when *in vitro* values fell within 2-fold of the observed *in vivo* data. Values above or below this threshold were determined to be overpredicted and underpredicted, respectively.

$$GMFE = 10^{\frac{\sum\left[log\frac{CL_{int,in\ vitro}}{CL_{int,in\ vivo}}\right]}{n}} \qquad \textbf{Equation 13}$$

$$RMSE = \sqrt{\frac{1}{n}\sum(predicted - observed)^2} \qquad \textbf{Equation 14}$$

Results

The diversity of drugs selected in this study (see Figure 1) resulted in a range of drug depletion-time profiles in both the media loss and conventional assays. All conventional assay profiles were observed to be monophasic, while those from the media loss assay were predominantly biphasic with a terminal phase parallel to the conventional assay profile. All time profiles under control conditions are displayed in Supplemental Figure 1 and representative examples are shown in Figure 3. Indinavir, midazolam and tolbutamide were exceptions showing monophasic profiles in both assays, indicating the importance of metabolism. A similar range of CL_{int} values were observed in both assay formats: 0.85 – 231 µL/min/mg protein in the media loss assay and 1.5 – 239 µL/min/mg protein in the conventional assay. However, the mean ratio of CL_{int} between the media loss and conventional assay for each compound was 2.81, indicating that clearance is typically greater in the media loss assay. Figure 4 shows the relationship between these two clearances for the 12 drugs studied, with the clearance ratio plotted against the media loss CL_{int} ($CL_{int,\ ML}$). Particularly high clearance ratios are evident for the four statins and valsartan. Both protease inhibitors, macrolides and repaglinide showed lower clearance ratios between 1.4-1.8 while for the two control compounds no difference was evident.

Inhibitors of both uptake and metabolism were investigated to determine the effect on depletion-time profiles and resulting CL_{int} for each of the drugs. Representative profiles for four drugs displaying different characteristics are displayed in Figure 3 with CL_{int} values and their change relative to control listed in Table 1 and Table 2 for the media loss and conventional assays, respectively. A complete set of profiles for all drugs is displayed in Supplemental Figures 2 and 3.

The inclusion of ABT had no effect on the initial uptake phase in the media loss assay, while a reduced rate of terminal decay caused by metabolism was evident. Generally this led to reduced CL_{int} in both assay formats, however effects tended to be greater in the conventional than the media loss assay. For compounds which are metabolised slowly or minimally (cerivastatin, rosuvastatin and valsartan) no difference was observed, while drugs known to be rapidly metabolised (for example saquinavir, repaglinide, indinavir and atorvastatin, each with metabolic clearances >100 mL/min/kg, see Figure 1) showed substantial inhibition in both formats.

Inhibition of active uptake with the inclusion of Rfc is evident from the concentration-time profiles of drugs relying predominantly on active transport for hepatocyte uptake, which resulted in reduced depletion over time in comparison to control conditions. The effect was more pronounced for the media loss assay. Control compounds and those with lower clearance ratios (clarithromycin, indinavir, saquinavir and erythromycin) were largely unaffected by the inclusion of Rfc. The anomalous result noted for tolbutamide was attributed to the low intrinsic clearance (<1 µL/min/mg protein) and the limited accuracy in this low region. Combination of ABT and Rfc typically had an additive inhibitory effect, causing a greater reduction of CL_{int} than observed for either Rfc or ABT alone to a similar extent in both formats.

Time profiles for all drugs in each assay format were analysed using a mechanistic model in order to obtain values for CL_{active}, $CL_{passive}$, CL_{met} and $V_{app,cell}$. The estimated values of these parameters are displayed in Table 3 (fitted concentration-time profiles are displayed in Supplemental Figures 4 and 5). The model parameters generally

matched the expected characteristics in terms of proportion of active transport and rate of metabolism. The range of CL_{active} and $CL_{passive}$ values was 40 and 120-fold, with valsartan lowest (18.1 and 3.2 µL/min/mg protein, respectively) and saquinavir highest (777 and 383 µL/min/mg protein, respectively) for both clearances. In the case of tolbutamide and midazolam, profiles were monophasic in all experimental conditions and hence the mechanistic model was not applied. CL_{met} showed a 70-fold range of values with valsartan (comparable with tolbutamide) and saquinavir (approaching midazolam) again being the extremes (2.2 and 139 µL/min/mg, respectively).

Linear regression analysis revealed three key relationships; a strong, significant relationship between Log $CL_{passive}$ and $LogD_{7.4}$ (r^2 = 0.69; p < 0.01; Figure 5A), and CL_{met} and $LogD_{7.4}$ (r^2 = 0.79; p < 0.01; Figure 5B). These relationships could be valuable for an initial estimation of the importance of metabolism and passive permeability using the $LogD_{7.4}$. Also, unexpectedly, CL_{active} and $CL_{passive}$ were found to be positively related (r^2 = 0.71; p < 0.01; Figure 5C).

Parameters Kp, Kp_u and fu_{cell} are also listed in Table 3. Kp and Kp_u ranged between 3.8 – 254 and 2.3 – 8.3 respectively (excluding tolbutamide and midazolam), and are indicative of the range of intracellular binding and active transport properties of the drugs selected in this study. From these values, estimates of fu_{cell} ranged between 0.014 – 0.263 for saquinavir and valsartan, respectively. Linear regression analysis indicated no relationship between either $CL_{passive}$, CL_{active} or Kp_u and the fu_{cell} for the 12 drugs investigated, confirming that intracellular binding was independent of uptake characteristics. Similarly Figure 5D illustrates the lack of any relationship between $V_{cell,app}$ and Kp_u.

To assess the utility of the current methodology as a predictor of *in vivo* clearance, parameters from both the direct cellular assay ($CL_{int,\ ML}$, see Table 1), and following mechanistic modelling (CL_{uptake} and CL_{met}, see Table 3) were evaluated. Clearance values were scaled to the level of the whole body using standard physiological scaling factors. Clearance values (Table 4) showed similar ranges: 6 – 1,851, 15 – 1,887 and 26 – 3,587 mL/min/kg for $CL_{int,ML}$, CL_{met} and CL_{uptake}, respectively.

In terms of *in vivo* clearance predictions, CL_{uptake} was seen to have least bias and precision according to the GMFE and RMSE values compared to CL_{met} and $CL_{int,ML}$ (Table 4). However, it is evident that the success of each parameter is drug dependent (Figure 6). Four of the five drugs with high clearance ratios (all of which were statins) were best predicted by CL_{uptake}; valsartan, the other high clearance ratio drug, was not well predicted by any of the clearance terms. For the five lower clearance ratio drugs, $CL_{int,ML}$ was the most successful predictor, however in the case of repaglinide CL_{uptake} was comparable and for saquinavir and erythromycin CL_{met} was comparable. Indinavir, the other member of this group, was not well predicted by any of the clearance terms. The control drugs were also best predicted by the $CL_{int,ML}$ or the CL_{met} parameters. This highlights the difficulty in the application of a generic cellular extrapolation approach if the properties of the compound are not considered. Of the three terms, $CL_{int,ML}$ produced the highest frequency of predictions within 2-fold of the observed *in vivo* clearance (58% compared to 50% and 33% for CL_{uptake} and CL_{met}, respectively). Values and trends for CL_{int} from the conventional assay were almost identical to CL_{met}, and so are not presented.

Discussion

In this study the methodology of the media loss assay previously proposed (Jigorel and Houston, 2012, Soars et al., 2007) was adapted to increase throughput and also to be more informative through the use of inhibitors. It was anticipated that this approach would allow implementation of a simple mechanistic model to estimate values for several clearance processes (active, passive and metabolic), as well as providing information on intracellular binding and partitioning of the drug. The use of multi well plates not only reduces the demands of the required reagents and operator time, but also increases the feasibility of simultaneously investigating multiple experimental conditions, as exemplified here with the use of various inhibitor conditions.

Drugs in this study were selected to represent a range of metabolic clearances and relative contributions of active and passive transport, as determined from previous *in vitro* data (see Figure 1). Comparison of time profiles obtained from the conventional and media loss assay served to highlight the clear differences between assays. While all conventional depletion assays were monophasic, the majority of media loss profiles were biphasic, indicating that uptake occurred at a different rate to that of the subsequent metabolism. Indinavir and the control compounds (midazolam and tolbutamide) were exceptions, with monophasic profiles observed in both assays under basal conditions. While it was expected for both midazolam and tolbutamide, selected as low and high clearance drugs with minimal transporter involvement, it was unexpected for indinavir, which had been shown previously to be transported predominantly by an active process (De Bruyn et al., 2016). Drugs with a small passive permeability component displayed high clearance ratios (higher CL_{int} in the media loss,

compared to the conventional depletion), and were also the most affected by Rfc, confirming the importance of uptake to their hepatic clearance. In contrast those with lower clearance ratios (CL_{int} comparable across formats) reflected higher passive permeabilities and indicated that metabolism was the key determinant of their respective hepatic clearance.

The inclusion of inhibitors was intended to allow the estimation of individual clearance processes using a simple mechanistic model. ABT, a broad spectrum P450 inhibitor, was used in an attempt to prevent the majority of phase I metabolism, leaving the total rate of uptake as the key determinant of depletion rate. In both assay formats ABT reduced the depletion rate, indicating that it successfully inhibited a large degree of metabolism. However there is the obvious caveat that non P450 enzymes would not be susceptible to ABT. Inhibition caused by ABT only affected the terminal phase in the media loss assay, leaving the initial uptake phase unhindered. This method may be suitable as a standalone assay if a measure of total uptake alone was desired through the initial depletion phase. Rfc, a potent OATP inhibitor, was used to prevent active transport of drugs into the hepatocytes. The concentration used in this study has been shown previously to extensively inhibit rat Oatp1, Oatp2 and Ntcp (Fattinger et al., 2000). For the highly transported compounds (with high clearance ratios), Rfc greatly reduced the uptake phase in the media loss assay, while lower assay clearance ratio compounds appeared to be less affected. For indinavir, clarithromycin and repaglinide, it is unclear why Rfc had little effect, as previous data would suggest that these are subjected to active transport (De Bruyn et al., 2016, Menochet et al., 2012, Yabe et al., 2011). It is possible that activity of other transporters not inhibited by Rfc may enable continued uptake of these particular drugs. The control compounds

were largely unaffected by the inclusion of Rfc, consistent with the expectation that they enter the cell via passive diffusion. The effect of Rfc was also evident in the conventional depletion assay, which saw reduced clearance for several transported compounds. This is a secondary effect, since drug is prevented from entering the cells, thereby limiting the sequential metabolism. As anticipated the use of both inhibitors together generally led to an increase in inhibition compared to use of inhibitors individually. It should be noted that the current methodology would require modification for compounds that are non P450 or non OATP substrates, for example compounds that undergo extensive glucuronidation. In such cases, additional or alternative inhibitors would be required, however the same principles and model would apply.

Fitting of the mechanistic hepatocyte model followed a stepwise approach. First, data from the conventional depletion assay was modelled to give estimates of metabolic clearance and the interaction of inhibitors. This was then entered into the mechanistic model to allow the estimation of active transport, passive diffusion and an apparent volume of distribution using data from the media loss assay. Data typically followed the expected characteristics based on previous discussion, in terms of the proportions of active transport and metabolism. Once again the outliers were indinavir, repaglinide and clarithromycin. It was also observed that in the case of midazolam and tolbutamide, where profiles remained monophasic under all experimental conditions, the mechanistic model became highly insensitive to changes in uptake parameters, and were hence excluded from detailed analysis. These findings are consistent with active transport being a negligible contributor to the overall uptake clearance of the two compounds.

A strong correlation existed between the $LogD_{7.4}$ and the log of the estimated $CL_{passive}$ and CL_{met}. This relationship has been noted previously by Yabe et al. (2011) for $CL_{passive}$, and may serve as a useful tool for providing initial estimates of both passive diffusion and metabolic clearance for novel compounds, should the $LogD_{7.4}$ be known. A significant relationship was also observed between CL_{active} and $CL_{passive}$; a similar trend was reported by Yabe et al. (2011), although it did not reach statistical significance. These relationships could prove useful in assay design and data modelling for novel compounds for which little information is known.

Using the uptake terms (CL_{active} and $CL_{passive}$), along with the $V_{cell, app}$ estimated in the mechanistic model, it was possible to indirectly determine the ratios of total and unbound drug in hepatocytes to that in the medium (Kp and Kp_u, respectively) and therefore the extent of intracellular binding. Kp values varied by >60-fold and reflects the difference in both active transport and intracellular binding that occurs for each drug. Kp_u, which reflects the degree of active transport, had much less variation, with a >3-fold range. The difference between these two parameters is accounted for by the extent of intracellular binding, reflected by the almost 20-fold range in fu_{cell}. Values and rank order of fu_{cell} were in good agreement with that published previously (Menochet et al., 2012, Yabe et al., 2011). These terms provide a detailed understanding of the specific intracellular processes that govern the hepatic disposition of each drug.

In vivo hepatic clearance predictions were performed to determine the utility of $CL_{int,ML}$, CL_{uptake} and CL_{met} as predictors of *in vivo* clearance, with bias and precision assessed by GMFE and RMSE, respectively. Overall, CL_{uptake} had the lowest bias compared to $CL_{int,ML}$ and CL_{met} (GMFE = 2.96, 3.13 and 6.40, respectively), however it was evident

that the accuracy of each term was linked to drug clearance ratio. High ratio compounds were more accurately predicted when using CL_{uptake}, since this appeared to be the predominant clearance process, while lower clearance ratio drugs benefitted from the use of $CL_{int,ML}$ and CL_{met}. In both ratio groups there was one example (indinavir and valsartan) where no accurate prediction was obtained from any clearance term. It must also be considered that the $CL_{int,ML}$ term, while producing slightly greater bias than modelled uptake data, can be estimated using only the media loss assay (without the requirement for a simultaneous conventional assay). This method may therefore be more suitable if a quantitative prediction of $CL_{int,in\ vivo}$ is the sole reason for performing the assay, since fewer reagents and analysis is required, at the expense of producing estimates of CL_{int} only.

Further investigations would be needed if the methodology is to be extended from fresh to rat cryopreserved hepatocytes or to other species, particularly human. While highly adaptable in terms of practical aspects, it may prove challenging to accurately determine clearance parameters for species where rates of either metabolism or uptake are significantly lower. Additional applications of the methodology may also include determination of K_m values, as demonstrated previously by Jigorel and Houston (2012), and drug interaction studies, allowing estimation of IC_{50} or K_i values.

In conclusion, this study adapted the media loss assay into a higher throughput format, allowing the inclusion of several inhibitor conditions in order to split the observed CL_{int} into individual clearance parameters. Using a mechanistic model, it was possible to directly estimate the rates of active transport, passive diffusion and metabolism, as well as the apparent volume of distribution of the cell, and subsequently Kp, Kp_u and

the fu_{cell}. Together, these provide a detailed account of the parameters governing drug hepatic disposition. Clearance data from the media loss assay, metabolism and uptake data were assessed as a predictor of *in vivo* clearance. It was found that the accuracy of each clearance term was strongly linked to the particular drug characteristics. CL_{int} values from the media loss assay alone remains a viable option for quantitative predictions of *in vivo* clearance, if no additional information is required.

Acknowledgements

The authors wish to thank Sue Murby and Dr. David Hallifax for valuable assistance with LC-MS/MS analysis.

Author Contributions

Participated in research design: Harrison, De Bruyn, Darwich, Houston.

Conducted Experiments: Harrison.

Performed data analysis: Harrison.

Wrote or contributed to the writing of the manuscript: Harrison, De Bruyn, Darwich, Houston

References

BERRY, M. N. & FRIEND, D. S. 1969. High-yield preparation of isolated rat liver parenchymal cells: a biochemical and fine structural study. *J Cell Biol,* 43**,** 506-20.

BOW, D. A., PERRY, J. L., MILLER, D. S., PRITCHARD, J. B. & BROUWER, K. L. 2008. Localization of P-gp (Abcb1) and Mrp2 (Abcc2) in freshly isolated rat hepatocytes. *Drug Metab Dispos,* 36**,** 198-202.

BROWN, H. S., CHADWICK, A. & HOUSTON, J. B. 2007. Use of isolated hepatocyte preparations for cytochrome P450 inhibition studies: comparison with microsomes for Ki determination. *Drug Metab Dispos,* 35**,** 2119-26.

CHU, X., KORZEKWA, K., ELSBY, R., FENNER, K., GALETIN, A., LAI, Y., MATSSON, P., MOSS, A., NAGAR, S., ROSANIA, G. R., BAI, J. P., POLLI, J. W., SUGIYAMA, Y., BROUWER, K. L. & INTERNATIONAL TRANSPORTER, C. 2013. Intracellular drug concentrations and transporters: measurement, modeling, and implications for the liver. *Clin Pharmacol Ther,* 94**,** 126-41.

DAVIES, B. & MORRIS, T. 1993. Physiological parameters in laboratory animals and humans. *Pharm Res,* 10**,** 1093-5.

DE BRUYN, T., AUGUSTIJNS, P. F. & ANNAERT, P. P. 2016. Hepatic Clearance Prediction of Nine Human Immunodeficiency Virus Protease Inhibitors in Rat. *J Pharm Sci,* 105**,** 846-53.

DE BRUYN, T., CHATTERJEE, S., FATTAH, S., KEEMINK, J., NICOLAI, J., AUGUSTIJNS, P. & ANNAERT, P. 2013. Sandwich-cultured hepatocytes: utility for in vitro exploration of hepatobiliary drug disposition and drug-induced hepatotoxicity. *Expert Opin Drug Metab Toxicol,* 9**,** 589-616.

FATTINGER, K., CATTORI, V., HAGENBUCH, B., MEIER, P. J. & STIEGER, B. 2000. Rifamycin SV and rifampicin exhibit differential inhibition of the hepatic rat organic anion transporting polypeptides, Oatp1 and Oatp2. *Hepatology,* 32**,** 82-86.

GIACOMINI, K. M., HUANG, S. M., TWEEDIE, D. J., BENET, L. Z., BROUWER, K. L., CHU, X., DAHLIN, A., EVERS, R., FISCHER, V., HILLGREN, K. M., HOFFMASTER, K. A., ISHIKAWA, T., KEPPLER, D., KIM, R. B., LEE, C. A., NIEMI, M., POLLI, J. W., SUGIYAMA, Y., SWAAN, P. W., WARE, J. A., WRIGHT, S. H., YEE, S. W., ZAMEK-GLISZCZYNSKI, M. J., ZHANG, L. & CONSORTIUM, I. T. 2010. Membrane transporters in drug development. *Nat Rev Drug Discov,* 9**,** 215-36.

GRIFFIN, S. J. & HOUSTON, J. B. 2005. Prediction of in vitro intrinsic clearance from hepatocytes: comparison of suspensions and monolayer cultures. *Drug Metab Dispos,* 33**,** 115-20.

HALLIFAX, D., FOSTER, J. A. & HOUSTON, J. B. 2010. Prediction of human metabolic clearance from in vitro systems: retrospective analysis and prospective view. *Pharm Res,* 27**,** 2150-61.

HALLIFAX, D. & HOUSTON, J. B. 2006. Uptake and intracellular binding of lipophilic amine drugs by isolated rat hepatocytes and implications for prediction of in vivo metabolic clearance. *Drug Metab Dispos,* 34**,** 1829-36.

HOUSTON, J. B. 1994. Utility of in vitro drug metabolism data in predicting in vivo metabolic clearance. *Biochem Pharmacol,* 47**,** 1469-79.

ITO, K. & HOUSTON, J. B. 2004. Comparison of the use of liver models for predicting drug clearance using in vitro kinetic data from hepatic microsomes and isolated hepatocytes. *Pharm Res,* 21**,** 785-92.

JIGOREL, E. & HOUSTON, J. B. 2012. Utility of drug depletion-time profiles in isolated hepatocytes for accessing hepatic uptake clearance: identifying rate-limiting steps and role of passive processes. *Drug Metab Dispos,* 40**,** 1596-602.

JIGOREL, E., LE VEE, M., BOURSIER-NEYRET, C., BERTRAND, M. & FARDEL, O. 2005. Functional expression of sinusoidal drug transporters in primary human and rat hepatocytes. *Drug Metab Dispos,* 33**,** 1418-22.

JONES, H. M., CHEN, Y., GIBSON, C., HEIMBACH, T., PARROTT, N., PETERS, S. A., SNOEYS, J., UPRETI, V. V., ZHENG, M. & HALL, S. D. 2015. Physiologically based pharmacokinetic modeling in drug discovery and development: a pharmaceutical industry perspective. *Clin Pharmacol Ther,* 97**,** 247-62.

MENOCHET, K., KENWORTHY, K. E., HOUSTON, J. B. & GALETIN, A. 2012. Simultaneous assessment of uptake and metabolism in rat hepatocytes: a comprehensive mechanistic model. *J Pharmacol Exp Ther,* 341**,** 2-15.

MIYAUCHI, S., SAWADA, Y., IGA, T., HANANO, M. & SUGIYAMA, Y. 1993. Comparison of the hepatic uptake clearances of fifteen drugs with a wide range of membrane permeabilities in isolated rat hepatocytes and perfused rat livers. *Pharm Res,* 10**,** 434-40.

MUGFORD, C. A., MORTILLO, M., MICO, B. A. & TARLOFF, J. B. 1992. 1-Aminobenzotriazole-induced destruction of hepatic and renal cytochromes P450 in male Sprague-Dawley rats. *Fundam Appl Toxicol,* 19**,** 43-9.

NICHOLLS, G. & HOUSTON, J. B. 1996. Drug transport and binding in isolated hepatocytes: implications for intrinsic clearance determinations in hepatocytes and hepatic microsomes. *European Journal of Pharmaceutical Sciences,* 4**,** S196.

PAINE, A. J. 1990. The maintenance of cytochrome P-450 in rat hepatocyte culture: some applications of liver cell cultures to the study of drug metabolism, toxicity and the induction of the P-450 system. *Chem Biol Interact,* 74**,** 1-31.

SEGLEN, P. O. 1976. Preparation of isolated rat liver cells. *Methods Cell Biol,* 13**,** 29-83.

SHITARA, Y., HORIE, T. & SUGIYAMA, Y. 2006. Transporters as a determinant of drug clearance and tissue distribution. *Eur J Pharm Sci,* 27**,** 425-46.

SOARS, M. G., GRIME, K., SPROSTON, J. L., WEBBORN, P. J. & RILEY, R. J. 2007. Use of hepatocytes to assess the contribution of hepatic uptake to clearance in vivo. *Drug Metab Dispos,* 35**,** 859-65.

WOOD, F. L., HOUSTON, J. B. & HALLIFAX, D. 2017. Clearance prediction methodology needs fundamental improvement: trends common to rat and human hepatocytes/microsomes and implications for experimental methodology. *Drug Metab Dispos*.

YABE, Y., GALETIN, A. & HOUSTON, J. B. 2011. Kinetic characterization of rat hepatic uptake of 16 actively transported drugs. *Drug Metab Dispos,* 39**,** 1808-14.

ZAMEK-GLISZCZYNSKI, M. J., LEE, C. A., POIRIER, A., BENTZ, J., CHU, X., ELLENS, H., ISHIKAWA, T., JAMEI, M., KALVASS, J. C., NAGAR, S., PANG, K. S., KORZEKWA, K., SWAAN, P. W., TAUB, M. E., ZHAO, P., GALETIN, A. & INTERNATIONAL TRANSPORTER, C. 2013. ITC recommendations for transporter kinetic parameter estimation and translational modeling of transport-mediated PK and DDIs in humans. *Clin Pharmacol Ther,* 94**,** 64-79.

Footnote

This work was supported by a consortium of pharmaceutical companies (GlaxoSmithKline, Lilly and Pfizer) within the Centre for Applied Pharmacokinetic Research at the University of Manchester.

Figure Legends

Figure 1 - Kp_u plotted against CL_{met} for 17 drugs in rat hepatocytes. Data were taken from literature (see Supplemental Table 1). CL_{met} data were scaled using standard physiological scaling factors of 200 mg protein/g liver and 40 g liver/kg bodyweight. Drugs are identified as follows: 1) Amprenavir, 2) Atazanavir, 3) Atorvastatin, 4) Bosentan, 5) Cerivastatin, 6) Clarithromycin, 7) Darunavir, 8) Erythromycin, 9) Fexofenadine, 10) Indinavir, 11) Indomethacin, 12) Pitavastatin, 13) Repaglinide, 14) Ritonavir, 15) Rosuvastatin, 16) Saquinavir, 17) Valsartan. Symbols in red represent those investigated in this study.

Figure 2 – Experimental and data analysis approaches. Panel A: Schematic outline of the approach taken for generating and modelling of data from both the media loss and conventional assay. Panel B: Two-compartment mechanistic model used to describe drug uptake (active and passive), metabolism and apparent cell volume.

Figure 3 – Representative substrate depletion-time profiles in rat hepatocytes at 1 µM, with data fitted using Equation 1 Equation 2. Media Loss and Conventional assay are displayed, respectively, for atorvastatin (A-B), pitavastatin (C-D), saquinavir (E-F) and tolbutamide (G-H). Data were generated using the media loss assay or the conventional depletion assay. Observed data (●) represents mean ± SD (n=3).

Figure 4 – Media loss CL_{int} ($CL_{int, ML}$) plotted against the ratio between $CL_{int,ML}$ and CL_{int} measured in the conventional assay, calculated using Equation 3 and Equation 4 as appropriate. Drugs are identified as follows: 1) Atorvastatin, 2) Cerivastatin, 3) Clarithromycin, 4) Erythromycin, 5) Indinavir, 6) Midazolam, 7) Pitavastatin, 8) Repaglinide, 9) Rosuvastatin, 10) Saquinavir, 11) Tolbutamide, 12) Valsartan. Values close to unity denote no difference between assay formats and a clearance ratio of 2 is shown as a distinction for high and low ratios between assay formats.

Figure 5 – Uptake and metabolism characteristics calculated for 12 drugs using data from rat media loss and conventional depletion assays, entered into a mechanistic cell model. Relationship between $LogD_{7.4}$ and Log $CL_{passive}$ (A), $LogD_{7.4}$ and Log CL_{met} (B), *in vitro* CL_{active} and $CL_{passive}$ (C) and $V_{cell,app}$ and Kp_u (D). The solid line in panels A, B and C represents linear line of best fit, described by Log $CL_{passive}$ = 0.25 $LogD_{7.4}$ + 1.08, Log CL_{met} = 0.37 $LogD_{7.4}$ + 0.51 and Log $CL_{passive}$ = 0.89 Log CL_{active} - 0.24, respectively.

Figure 6 - Observed $CL_{int,\ in\ vivo}$ plotted against $CL_{int,ML}$ (A), CL_{met} (B) and CL_{uptake}(C) scaled using standard physiological scaling factors of 200 mg protein/g liver and 40 g liver/kg bodyweight. Drugs are identified as follows: 1) Atorvastatin, 2) Cerivastatin, 3) Clarithromycin, 4) Erythromycin, 5) Indinavir, 6) Midazolam, 7) Pitavastatin, 8) Repaglinide, 9) Rosuvastatin, 10) Saquinavir, 11) Tolbutamide, 12) Valsartan. Line of unity (solid line), and 2-fold under and over-prediction (dashed line) are displayed.

Table 1 - CL_{int} values and the percentage of control values, determined in the media loss assay in the presence of ABT and/or Rfc. Data represents mean ± SD (n=3).

Media Loss							
Drug	CL_{int} (µL/min/mg protein)				% of control		
	Control	ABT	Rfc	ABT+Rfc	ABT	Rfc	ABT+Rfc
Atorvastatin	120 ± 18.9	45.9 ± 7.0	7.1 ± 4.8	4.6 ± 1.0	38*	6*	4*
Cerivastatin	47.1 ± 13.9	30.7 ± 16.5	15.0 ± 2.2	9.7 ± 3.0	65	32*	21*
Clarithromycin	16.2 ± 3.4	7.2 ± 2.4	17.8 ± 3.0	5.0 ± 3.4	45*	110	31*
Erythromycin	16.2 ± 6.7	5.1 ± 1.4	13.1 ± 4.4	3.9 ± 1.5	32*	81	24*
Indinavir	80.4 ± 17.5	12.2 ± 3.3	56.4 ± 22.1	10.9 ± 4.6	15*	70	14*
Midazolam	231 ± 67	32.3 ± 6.5	288 ± 28	33.3 ± 12.2	14*	125	14*
Pitavastatin	32.5 ± 1.3	15.1 ± 9.0	2.1 ± 1.8	1.9 ± 1.6	46*	7*	6*
Repaglinide	44.2 ± 11.3	11.8 ± 0.4	17.1 ± 6.8	7.6 ± 3.2	27*	39*	17*
Rosuvastatin	6.5 ± 5.2	6.5 ± 3.4	1.3 ± 0.9	1.3 ± 0.4	99	19	20
Saquinavir	112 ± 28	33.3 ± 13.3	97.1 ± 28.4	28.1 ± 9.3	30*	87	25*
Tolbutamide	0.85 ± 0.39	0.84 ± 0.52	1.61 ± 0.47	0.87 ± 0.48	99	189	102
Valsartan	5.8 ± 3.2	8.0 ± 2.6	1.7 ± 0.5	1.7 ± 1.0	137	29	29

* denotes a p value of < 0.05 using Scheffe's test following ANOVA

Table 2 - CL_{int} values and the percentage of control values, determined in the conventional depletion assay in the presence of ABT and/or Rfc. Data represents mean ± SD (n=3).

	Conventional						
Drug	CL_{int} (µL/min/mg protein)				% of control		
	Control	ABT	Rfc	ABT+Rfc	ABT	Rfc	ABT+Rfc
Atorvastatin	42.6 ± 7.9	9.8 ± 0.8	8.1 ± 2.1	2.3 ± 1.4	23*	19*	5*
Cerivastatin	4.9 ± 2.7	1.2 ± 1.2	5.7 ± 1.5	1.2 ± 1.3	25	118	26
Clarithromycin	9.1 ± 0.3	0.5 ± 0.5	8.2 ± 1.5	0.3 ± 0.3	6*	90	4*
Erythromycin	11.4 ± 2.2	1.4 ± 0.6	7.1 ± 2.0	0.4 ± 0.3	12*	62*	4*
Indinavir	57.4 ± 13.5	6.4 ± 1.4	38.6 ± 4.9	5.5 ± 1.3	11*	67	10*
Midazolam	239 ± 14	7.1 ± 2.9	246 ± 36	8.0 ± 3.4	3*	103	3*
Pitavastatin	6.3 ± 1.1	0.9 ± 0.2	1.5 ± 0.7	0.4 ± 0.2	14*	25*	6*
Repaglinide	24.8 ± 8.4	8.0 ± 2.6	13.5 ± 6.5	4.2 ± 1.7	32*	54	17*
Rosuvastatin	2.2 ± 0.5	2.2 ± 0.4	0.8 ± 0.2	0.8 ± 0.6	97	36*	36*
Saquinavir	73.8 ± 17.9	18.0 ± 3.5	53.2 ± 13.7	16.6 ± 3.1	24*	72	22*
Tolbutamide	1.83 ± 0.40	0.81 ± 0.44	1.46 ± 0.56	0.44 ± 0.35	44	80	24*
Valsartan	1.5 ± 0.7	1.9 ± 1.7	0.5 ± 0.7	0.09 ± 0.02	125	33	6

* denotes a p value of < 0.05 using Scheffe's test following ANOVA

Table 3 – Summary of uptake, metabolism, distribution and binding parameters calculated using a mechanistic model. Results are displayed as the mean ± SD (n=3).

Drug	CL_{met}	CL_{uptake}	CL_{active}	$CL_{passive}$	% active transport	$V_{cell,app}$	Kp	Kp_u	fu_{cell}
	µL/min/mg					µL/mg protein			
Atorvastatin	34.0 ± 9.7	208 ± 34.2	183 ± 33.5	25.1 ± 7.1	88	1.0 ± 0.3	65.0	8.3	0.128
Cerivastatin	4.8 ± 2.7	167 ± 67.8	136 ± 66.6	30.8 ± 12.6	82	386 ± 287	254	5.4	0.021
Clarithromycin	8.7 ± 0.5	46.3 ± 9.5	26.3 ± 8.7	20.0 ± 3.8	57	130 ± 8.8	73.5	2.3	0.031
Erythromycin	12.4 ± 4.0	48.4 ± 8.6	28.9 ± 7.6	19.5 ± 4.0	60	24.8 ± 20.8	16.4	2.5	0.151
Indinavir	52.5 ± 9.7	143 ± 41.2	87.0 ± 38.6	56.1 ± 14.6	61	3.6 ± 5.5	3.8	2.6	0.666
Pitavastatin	6.7 ± 1.1	150 ± 56.4	125 ± 55.0	25.2 ± 12.5	83	60.9 ± 33.4	81.2	5.9	0.073
Repaglinide	25.8 ± 10.6	95.8 ± 19.0	59.2 ± 17.9	36.7 ± 6.3	62	52.1 ± 31.5	35.1	2.6	0.074
Rosuvastatin	2.3 ± 0.5	207 ± 64.3	161 ± 61.2	46.5 ± 19.8	78	54.8 ± 15.2	24.1	4.5	0.185
Saquinavir	139 ± 40.9	1160 ± 919	777 ± 866	383 ± 307	67	256 ± 188	221	3.0	0.014
Valsartan	2.2 ± 0.6	21.3 ± 3.3	18.1 ± 3.3	3.2 ± 0.5	85	31.1 ± 6.9	25.6	6.7	0.263

Table 4 – Assessment of accuracy and precision of $CL_{int,\ ML}$, CL_{met} and CL_{uptake} parameters for the prediction of *in vivo* clearance. Data were scaled using standard physiological scaling factors of 200mg protein/g liver and 40 g liver/kg bodyweight. For *in vivo* references, see Supplemental Table 2.

Drug	$CL_{int,\ ML}$	CL_{met}	CL_{uptake}	$CL_{int,\ in\ vivo}$	Predicted/Observed		
	mL/min/kg				$CL_{int,\ ML}$	CL_{met}	CL_{uptake}
Atorvastatin	960 ± 151	272 ± 77	1664 ± 274	1593	0.60	0.17	1.04
Cerivastatin	377 ± 111	38 ± 22	1333 ± 542	1517	0.25	0.03	0.88
Clarithromycin	129 ± 28	70 ± 3.7	371 ± 76	121	1.07	0.58	3.07
Erythromycin	129 ± 54	100 ± 32	387 ± 69	115.5	1.12	0.87	3.35
Indinavir	643 ± 140	420 ± 78	1145 ± 330	50	12.9	8.41	22.94
Midazolam	1851 ± 536	1887 ± 144[a]	-	1331	1.39	1.42	-
Pitavastatin	260 ± 10	54 ± 8.7	1201 ± 451	1165	0.22	0.05	1.03
Repaglinide	353 ± 90	206 ± 85	767 ± 152	496	0.71	0.42	1.55
Rosuvastatin	52 ± 42	19 ± 4.0	1658 ± 514	1412	0.04	0.01	1.17
Saquinavir	895 ± 221	1110 ± 327	9282 ± 7351	911	0.98	1.22	10.19
Tolbutamide	6.8 ± 3.1	15 ± 4.4[a]	-	7.4	0.92	1.96	-
Valsartan	47 ± 26	17 ± 5.1	171 ± 26	1554	0.03	0.01	0.11
				GMFE	3.13	6.41	2.94
				RMSE	779	915	2771

[a] Data calculated from conventional depletion assay using Equation 1

Figure 1

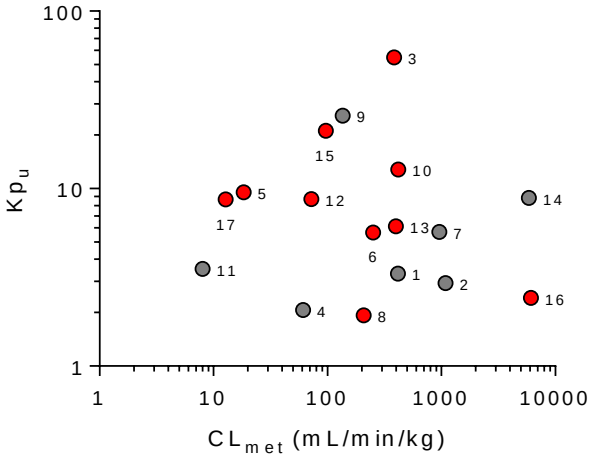
100
10
1
Kpu
1
10
100
1000
10000
CLmet (mL/min/kg)
3
9
15
10
5
12
14
17
13
7
6
11
1
2
16
4
8

Figure 2

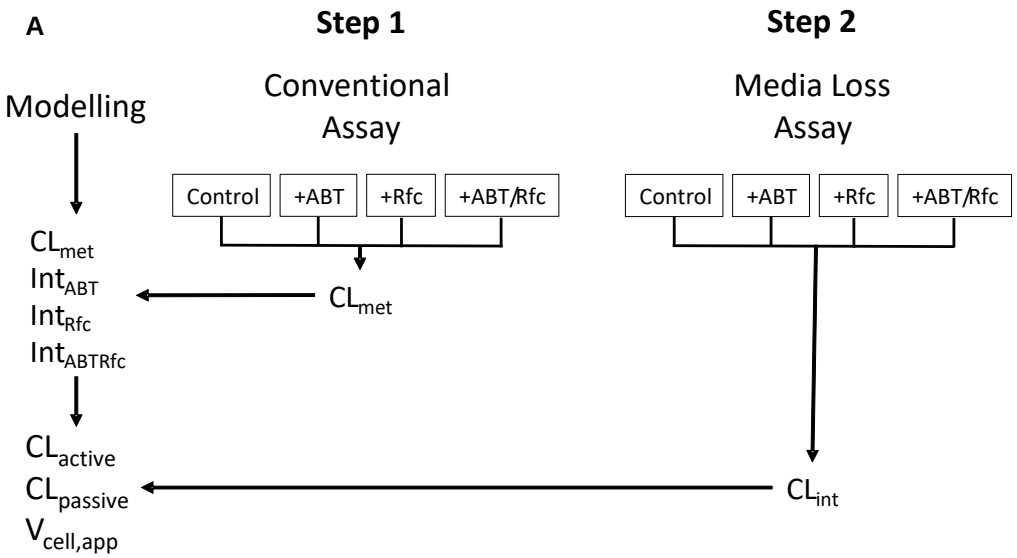
A
Step 1
Step 2
Modelling
Conventional Assay
Media Loss Assay
Control
+ABT
+Rfc
+ABT/Rfc
Control
+ABT
+Rfc
+ABT/Rfc
CLmet
IntABT
IntRfc
IntABTRfc
CLmet
CLactive
CLpassive
Vcell,app
CLint

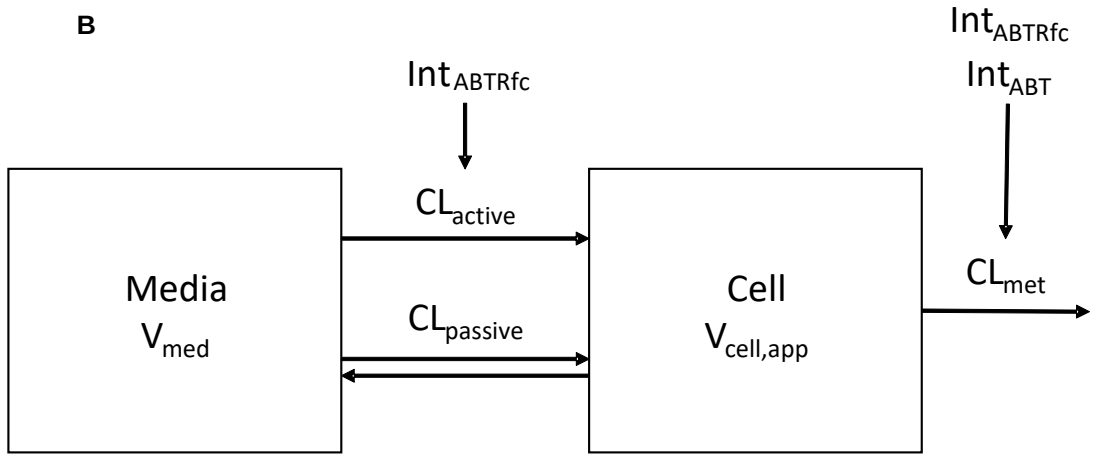
B
IntABTRfc
IntABTRfc
IntABT
CLactive
Media
Vmed
CLpassive
Cell
Vcell,app
CLmet

Figure 3

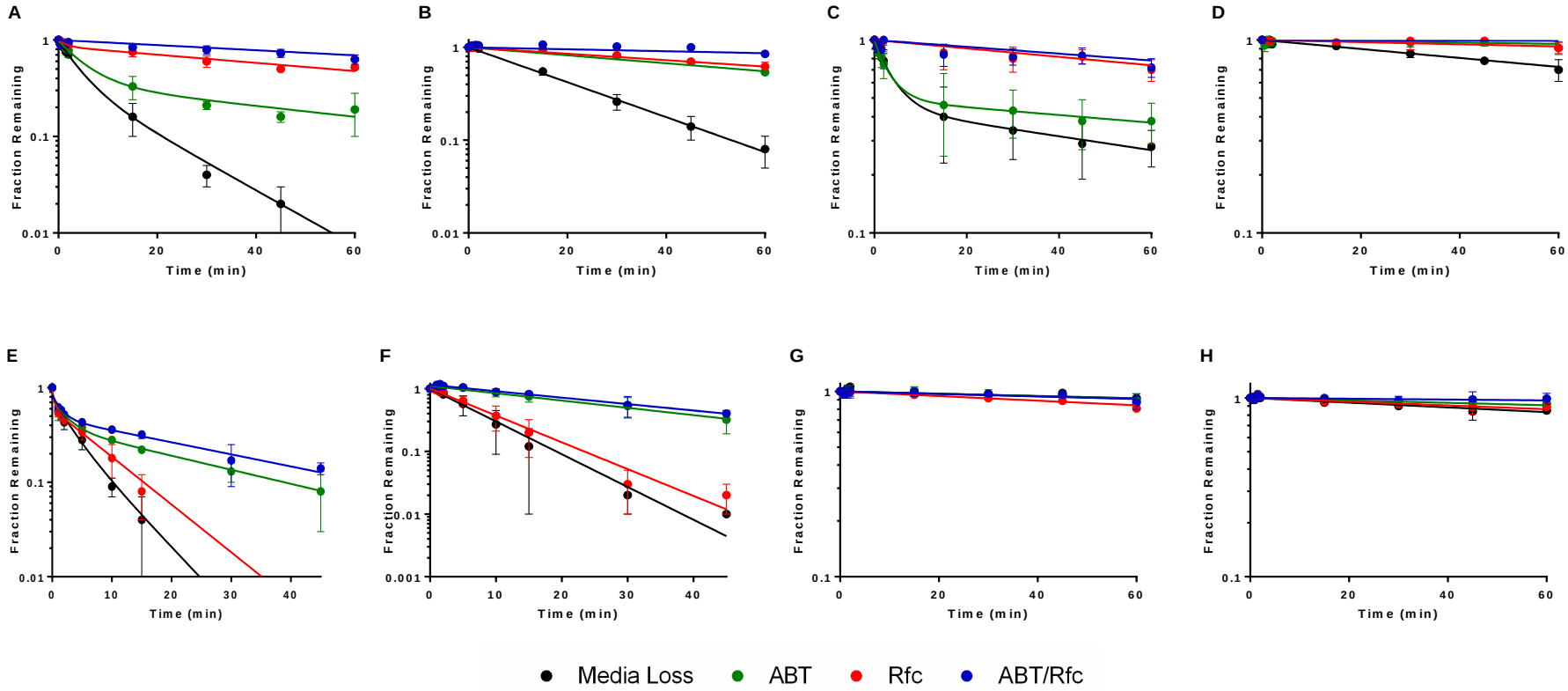
A
B
C
D
E
F
G
H
Fraction Remaining
Time (min)
Media Loss
ABT
Rfc
ABT/Rfc

Figure 4

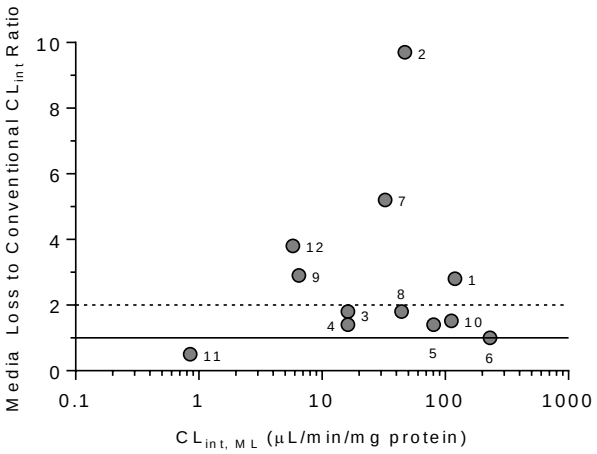
Media Loss to Conventional CL_{int} Ratio
10
8
6
4
2
0
0.1
1
10
100
1000
$CL_{int,\ ML}$ (µL/min/mg protein)
2
7
12
9
1
8
3
4
10
11
5
6

Figure 5

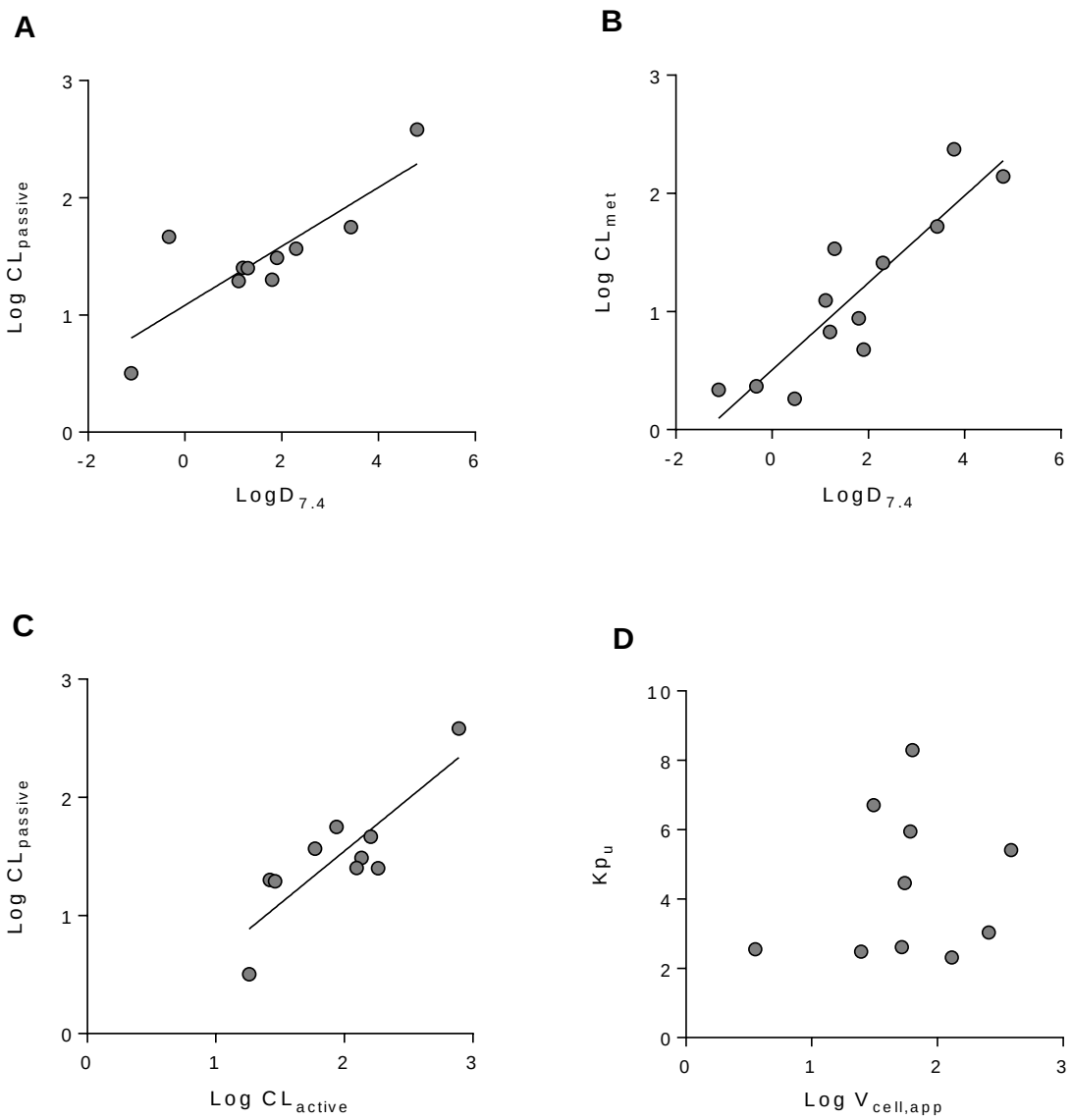
A
Log CL passive
LogD 7.4
B
Log CL met
LogD 7.4
C
Log CL passive
Log CL active
D
Kp u
Log V cell,app

Figure 6

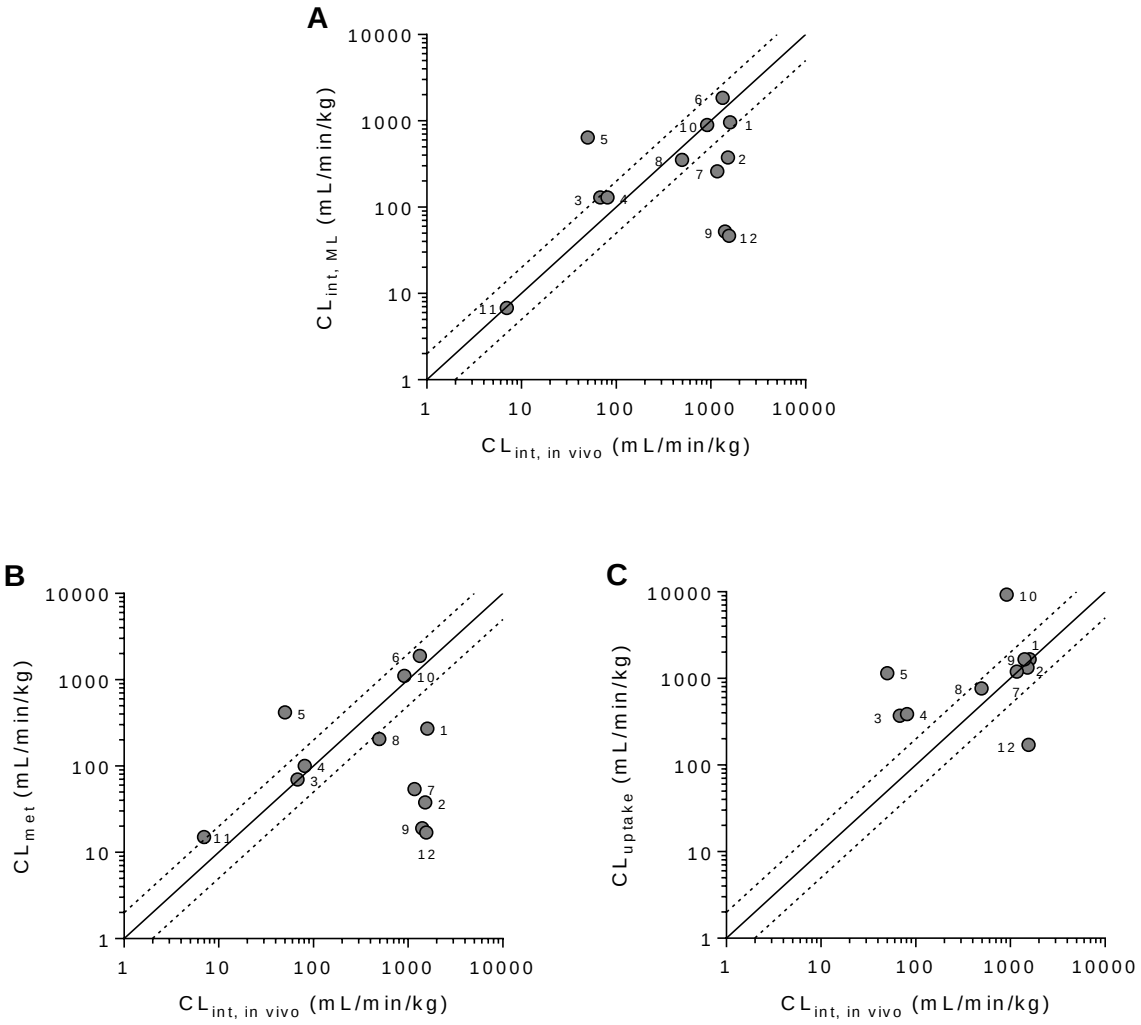
A
B
C
10000
1000
100
10
1
1
10
100
1000
10000
$CL_{int, ML}$ (mL/min/kg)
CL_{met} (mL/min/kg)
CL_{uptake} (mL/min/kg)
$CL_{int, in\ vivo}$ (mL/min/kg)